

Javier Fernández-Suárez · Fernando Corfu  
Ricardo Arenas · Alberto Marcos  
José R. Martínez Catalán · Florentino Díaz García  
Jacobo Abati · Francisco J. Fernández

## U–Pb evidence for a polyorogenic evolution of the HP–HT units of the NW Iberian Massif

**Abstract** A isotope dilution thermal ionisation mass spectrometry U–Pb geochronological study was carried out on the high-pressure and high-temperature units (HP–HT units) overlying the oceanic suture in the Allochthonous Complexes of the NW Iberian Variscan Belt. The rocks investigated are seven granulite- to eclogite-facies paragneisses and one leucosome within mafic high-pressure granulites in the Ordenes and Cabo Ortegal Complexes of NW Spain. U–Pb dating of zircon, monazite, titanite and rutile reveal the presence of a pervasive Early Ordovician metamorphic event at ca. 500–480 Ma and a later Early Devonian event at ca. 400–380 Ma. The U–Pb ages, in conjunction with petrological and structural data, indicate that the high-pressure event recorded by these rocks is Early Ordovician in age. Monazite ages in the paragneisses suggest that peak metamorphic conditions were reached at ca. 500–485 Ma. Subsequently, the rock ensemble underwent exhumation accompanied by partial melting and zircon growth at ca. 485–470 Ma. Melting of mafic granulites was coeval with this latter episode as indicated by zircon crystallisation age in the leucosomes dated at ca. 486 Ma. Based on these data and on the general features of magmatism and metamorphic evolution, it is proposed that this process took place at a convergent plate boundary within a peri-Gondwanan oceanic domain. Monazite, titanite and

rutile data in some of the samples studied show evidence of a second metamorphic episode that took place between ca. 400 and 380 Ma (with a peak at ca. 390–385 Ma). This Early Devonian event, at variance with the previous one, was not pervasive, but, rather, was localised in areas of intense Variscan tectonothermal reworking. It is claimed that this later metamorphic event was recorded by the U–Pb system in areas where monazite and titanite growth was enhanced by fluid circulation in highly strained rocks (Variscan shear zones). According to previous structural studies and Ar–Ar dating of fabrics, this Early Devonian episode took place as the HP–HT units were deformed and thrust upon the ophiolitic units in the early stages of the Variscan collision.

---

### Introduction

Lithospheric rocks that have been involved in more than one orogenic event have complex structural, metamorphic and isotopic features. This complexity is a result of the intricate interplay of the various tectonothermal events at different times and scales. One such example is found in the allochthonous high-pressure and high-temperature units (HP–HT units) overlying the Palaeozoic oceanic suture in the NW Iberian Massif. These rocks record the structural and metamorphic evolution related to the Variscan orogenic cycle, which was, in turn, superimposed on structures, fabrics and metamorphic features formed in an Early Palaeozoic geodynamic setting whose nature is still poorly constrained. The fact that the two sets of structural and metamorphic features obscure one another at all scales has created a debate on whether they formed in one or in the other orogenic cycle, an issue of crucial significance in deciphering the geological evolution of this rock ensemble.

Previous geochronological research on these HP–HT upper units has focused on the meta-igneous rocks (e.g. data compilation in Martínez Catalán et al. 1999). As a result of these investigations there is a general agreement on most, but not all, of the protolith ages of igneous rocks

---

J. Fernández-Suárez (✉) · R. Arenas · J. Abati  
Departamento de Petrología y Geoquímica,  
Universidad Complutense, 28040 Madrid, Spain  
E-mail: jfsuarez@geo.ucm.es

F. Corfu  
Mineralogical-Geological Museum,  
Universitet i Oslo, Sars gate 1, Oslo, Norway

A. Marcos · F.D. García · F.J. Fernández  
Departamento de Geología, Universidad de Oviedo,  
33005 Oviedo, Spain

J.R. Martínez Catalán  
Departamento de Geología, Universidad de Salamanca,  
37008 Salamanca, Spain

Editorial responsibility: T.L. Grove

and the ages of Variscan metamorphism. However, contention remains about the age of the HP HT event recorded by these rocks, precluding a time-integrated interpretation of their tectonothermal evolution. Geochronologic investigations in the HP HT units have so far yielded conflicting evidence regarding the age of the high-pressure event. Some data point to an Early Ordovician (ca. 490–480 Ma) age for this event (Kuijper 1979; Peucat et al. 1990) whilst other authors have furnished data suggesting an Early Devonian (ca. 405–380 Ma) age (Schäfer et al. 1993; Santos Zalduegui et al. 1996; Ordóñez Casado 1998). Recent geochronological investigations in intermediate-pressure, low to high-grade units (IP units) structurally overlying the HP HT units, have provided further evidence pointing to the existence of an Early Ordovician metamorphic event (Abati et al. 1999).

The aim of this study is to shed some light into the debate by means of a geochronological approach focused on the U–Pb systematics of accessory minerals in metasedimentary rocks belonging to the HP HT upper units. The study is based on the fact that the behaviour of the U–Pb system in accessory minerals is intimately related to the tectonothermal evolution of their host rocks and, therefore, will provide data that can be used, in conjunction with petrological and structural information, to obtain a clearer picture of their evolution. This relationship is, however, not straightforwardly interpretable as the factors controlling the behaviour and preservation of the U–Pb system in metamorphic rocks are multifarious and locally variable. The essential idea is thus to evaluate the new U–Pb data in the light of known aspects of the behaviour of the U-bearing minerals (zircon, monazite, titanite and rutile in the present case) and the pertinent structural and metamorphic data. This work is ultimately aimed at obtaining information regarding these issues: (1) to establish the nature of the events recorded by the U–Pb system and their time span, (2) to constrain the age of the oldest event recorded by these rocks, (3) to ascertain the age of the HP HT event and (4) to evaluate the Variscan tectonothermal overprint as reflected by the U–Pb system. In summary, the main scope of this work is to investigate the geochronological framework of the tectonothermal evolution of the units in the hanging wall to the Variscan suture in NW Iberia.

### **Geological setting: the NW Iberian Allochthonous Complexes**

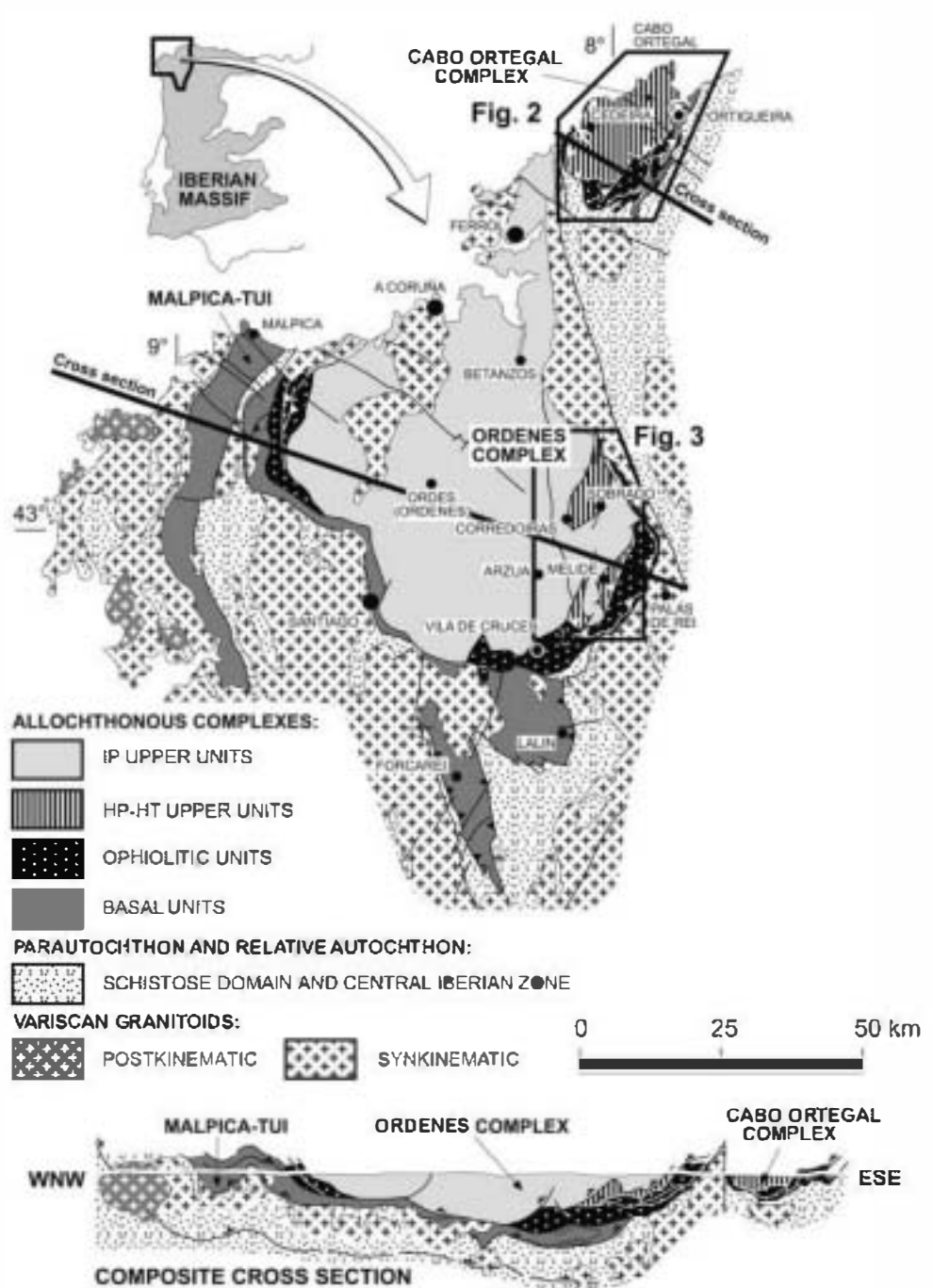
The geology of the NW Iberian allochthonous terranes has been the object of numerous studies during the past two decades (see review in Martínez Catalán et al. 1999, and references therein). Exposures of these terranes (known as Allochthonous Complexes) are found in five areas of north-west Spain (Cabo Ortegal, Ordenes and Maplica-Tui; Fig. 1) and north Portugal (Morais and Bragança). The Allochthonous Complexes (AC) consist of units stacked upon a relative autochthon considered to represent the continental margin of Gondwana. The

stacking of these units took place during the early stages of the Variscan orogeny. The AC were dismembered and thinned during their emplacement and exhumation (Martínez Catalán et al. 1996, 1999) and in the present day outcrop they are exposed as megaklippen with an internal megastructure of synforms or structural basins (Fig. 1).

The units that make up the AC have been classified into three groups according to their position in the original nappe pile: basal, intermediate (ophiolitic) and upper units (Figs. 2 and 3). The intermediate units are composed of massive metavolcanics, pillow breccias, metadiabases, metagabbros, plagiogranites, ultramafics, amphibolites, greenschists and minor metasediments that have been interpreted as a structurally dismembered ophiolitic sequence representing the oceanic suture in this realm of the Variscan belt (Martínez Catalán et al. 1997; Díaz García et al. 1999b). The basal units, structurally underlying the ophiolites, are composed of paragneisses, schists and mafic and felsic meta-igneous rocks (the latter including peralkaline granitoids). These units were affected by a Variscan high-pressure, low to intermediate-temperature metamorphism. Taking into account their lithological constitution and tectonothermal evolution, the basal units are considered to represent the external edge of the Gondwana margin that underwent crustal subduction at ca. 380–375 Ma under an accretionary wedge formed by the ophiolites and the upper units (Arenas et al. 1995, 1997; Martínez Catalán et al. 1996, 1999). The upper units, structurally overlying the suture, have been subdivided into two ensembles according to their metamorphic features: high-pressure and high-temperature units, occupying the lower structural position; and intermediate-pressure units in the uppermost structural position (Figs. 2 and 3).

The HP HT units, the objective of the present geochronological study, are composed of paragneisses, and mafic and ultramafic meta-igneous rocks. The most characteristic rocks are metabasites, commonly garnet-clinopyroxene granulites and eclogites, variably retrograded to the amphibolite facies (Vogel 1967). Gabbros occur in several stages of transformation, from virtually undeformed rocks scarcely affected by metamorphism, to coronitic metagabbros and HP granulites (Martínez Catalán and Arenas 1992; Arenas and Martínez Catalán 2000). In the less deformed gabbros, subophitic and diabase textures have been preserved, indicating an emplacement at relatively shallow levels. The geological setting of the mafic magmatism is not well constrained. In the Cabo Ortegal Complex, Peucat et al. (1990) considered the geochemistry of the mafic granulites to be similar to that of volcanic arc basalts, whereas the geochemical features of the eclogites are similar to those of N-type MORB rocks. Nevertheless, an origin as continental tholeiites has also been suggested for the metabasites of the same complex (Galán and Marcos 1997). Paragneisses are typically migmatitic and, according to the metamorphic characteristics of their mafic inclusions, they are either eclogitic or granulitic in origin (Vogel 1967). Finally, the ultramafic rocks include a heterogeneous ensemble of

Fig. 1. Map and composite cross section showing the main geological features of the Allochthonous Complexes in NW Spain



harzburgites, dumites and garnet pyroxenites for which an oceanic affinity has been proposed (Girardeau and Gil Ibarguchi 1991). The peak metamorphic conditions attained by the HP HT unit range from 9 to 18 kbar and 700 to 850 °C (Gil Ibarguchi et al. 1990; Arenas and Martínez Catalán 1993; Mendia 1996; Galán and Marcos 2000).

The IP units occupy the uppermost structural position in the nappe pile. They are composed of a thick sequence of terrigenous metasediments and large bodies of amphibolites, granitoid orthogneisses and gabbros. The metamorphism ranges from the greenschist facies in the uppermost part to the intermediate-pressure granulite facies in the lower part (ca. 7–10 kbar and 725–850 °C,

Abati 2000). The contact separating the IP units from the underlying HP HT units has been interpreted as an extensional structure, the Corredoiras Detachment (Martínez Catalán and Arenas 1992; Díaz García et al. 1999a). Current hypotheses for the geodynamic evolution of the upper units (Martínez Catalán et al. 1997, 1999) involve their genesis within the Rheic Ocean realm, followed by accretion to the wedge developed at the southern margin of the Avalon terrane in Late Ordovician–Early Silurian times. The subsequent convergence and collision between Laurentia and Gondwana Armorica, resulting in the closure of the Rheic ocean, caused the emplacement of the upper units over the ophiolitic units at ca.



HP-HT UNIT OF THE CABO ORTEGAL COMPLEX  
(Cabo Ortegal Nappe)

Fig. 2. Map and cross section of the Cabo Ortegal Complex showing the main geological units and the location of samples GCH-99-1, -6, -7 and -9

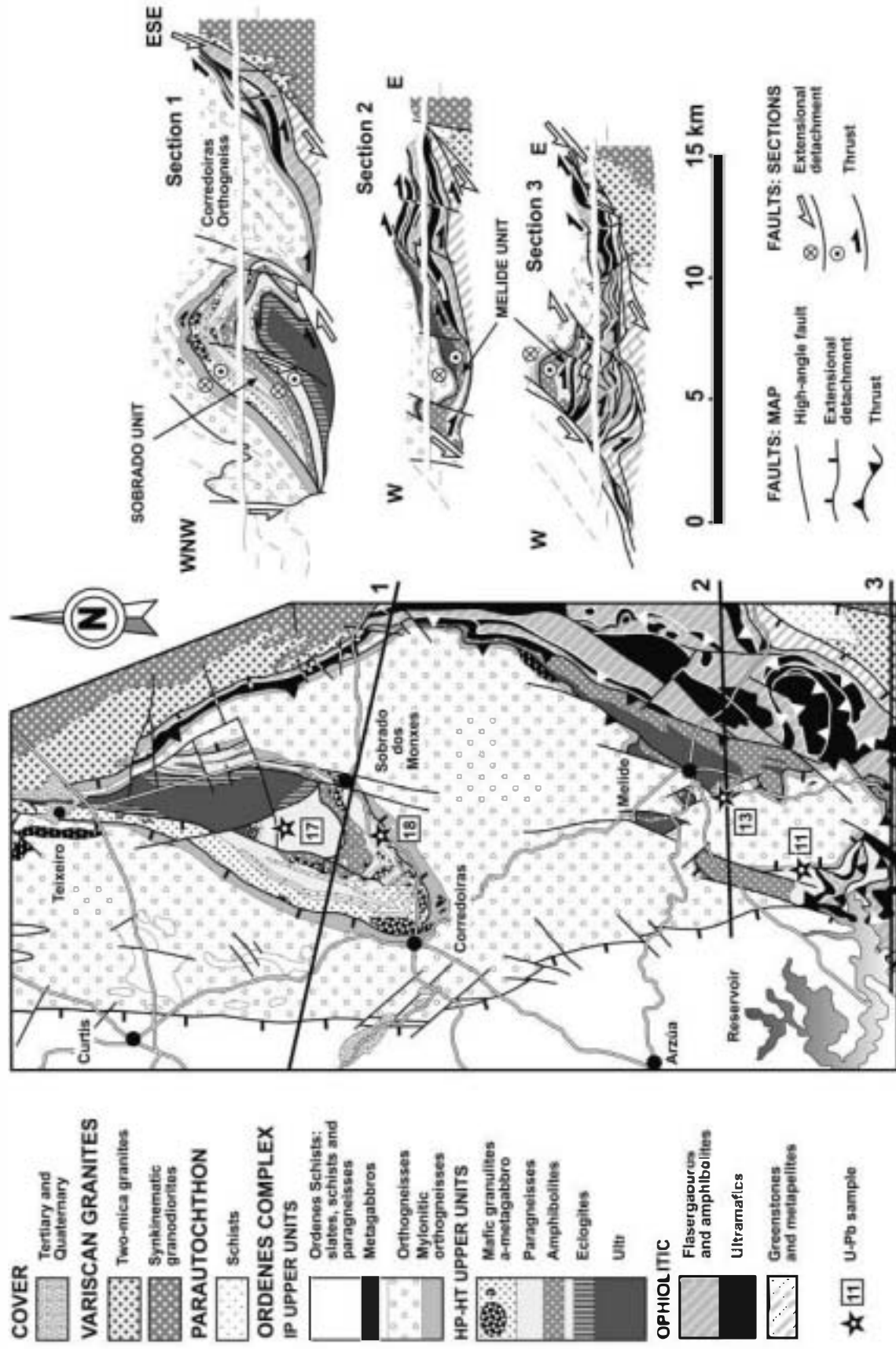


Fig. 3. Map and cross section of the eastern part of the Ordenes Complex showing the main units described in the text and the location of samples GCH-99-11, -13, -17 and -18



## Geochronological background of the upper units

Available geochronological data cover a variety of rocks from the five AC exposed in NW Iberia and were obtained by different methods (U Pb both thermal ionisation mass spectrometry (IDTIMS) and SHRIMP, Sm Nd, Rb Sr and Ar Ar). A compilation of published geochronological data on these units can be found in Martínez Catalán et al. (1999). What follows is a summary of the most important U Pb data obtained in rocks belonging to the units overlying the Variscan suture. In the HP HT units, geochronological research has focused on rocks of igneous origin: mafic granulites, eclogites and ultramafics. IDTIMS zircon U Pb data on eclogites and mafic granulites from the Cabo Ortegal and Ordenes complexes yielded ages in the range 480–490 Ma (Peucat et al. 1990). On the basis of the features of the zircon data, the authors suggested that this age dates a high-grade metamorphic event possibly occurring very shortly after the formation of the magmatic protoliths. SHRIMP U Pb data on allegedly magmatic domains of zircons from the HP mafic granulites (Schäfer et al. 1993; Ordóñez Casado 1998) yielded ages in the range 480–500 Ma, which are considered by the authors to represent the crystallisation age of the igneous protoliths. Younger ages are not reported in rims of the same zircons. U Pb ages for eclogite zircons are  $512 \pm 11$ ,  $495 \pm 11$  and  $469 \pm 9$  Ma, and their rims range between 380 and 390 Ma. The authors contend that the older ages represent protolith ages whereas the Devonian ages represent new zircon crystallisation under HP conditions and propose that a single subduction event at ca. 380–390 Ma caused the HP HT metamorphism recorded in these units. Within ultramafic bodies, the U Pb ages (both IDTIMS and SHRIMP) reported for pyroxenite veins and pegmatoids (Schäfer et al. 1993; Santos Zalduegui et al. 1996; Ordóñez Casado 1998) range between ca. 385 and 395 Ma. These ages are interpreted to date an Early Devonian episode of mantle melting at high pressure conditions. Ages on paragneisses from the HP HT units are scarcer. IDTIMS U Pb data for Cabo Ortegal paragneisses (Peucat et al. 1990) yielded lower intercept ages of  $417 \pm 3/2$  and  $422 \pm 4$  Ma. Kuijper (1979) studied a sample of migmatitic paragneisses from the Ordenes Complex and obtained a lower intercept zircon age of  $476 \pm 12$  Ma and a sub-concordant monazite fraction with a  $^{207}\text{Pb}/^{206}\text{Pb}$  age of 487 Ma. SHRIMP data on zircons from the eclogite-facies Chimparra Gneiss (Cabo Ortegal Complex; Ordóñez Casado 1998) have yielded primary ages spreading from ca. 515 up to ca. 2.14 Ga. Analyses on zircon rims interpreted as metamorphic overgrowths yielded ages of around 390 Ma.

Within the IP units, U Pb (IDTIMS) zircon data from intrusive gabbros and granitoids indicate crystallisation ages of ca. 495–500 Ma (Dalhner and Tucker 1993;

Abati et al. 1999). Within the same units, Abati et al. (1999) obtained concordant monazite ages in granulite-facies paragneisses in the range 493–498 Ma and they found no isotopic evidence for younger events in the samples investigated, with the exception of two rutile fractions yielding  $^{206}\text{Pb}/^{238}\text{U}$  ages at ca. 380–390 Ma.

## Sampling rationale and sample description

Considering the results of previous geochronological investigations and based on the present knowledge of the tectonic and metamorphic history of the area, we studied seven samples representing the high-grade (granulite- to eclogite-facies) paragneisses exposed in the Cabo Ortegal and Ordenes Complexes (Figs. 2 and 3). Dating of paragneisses circumvents the controversy between protolith vs metamorphic age that has been a recurrent issue in the interpretation of U Pb data in the meta-igneous rocks from these units (cf. Peucat et al. 1990; Ordóñez Casado 1998). A valuable additional constraint on the age of the HP HT event can be provided by the crystallisation age of leucosomes associated with HP mafic granulites, whose field relationships indicate a formation broadly coeval with the development of the retrogressive fabric associated with the granulites. For that purpose we studied one sample of such leucosomes within mafic granulites of the Cabo Ortegal Complex.

A description of the salient petrological features of the samples investigated (location in Figs. 2 and 3) is given below.

### Cabo Ortegal Complex

#### *GCH-99-1: Banded Gneiss; Grt Sil-bearing biotitic paragneiss*

The Banded Gneiss Formation (Vogel 1967; Fig. 2) is constituted by pelitic to semi-pelitic migmatitic gneisses with a complex tectonothermal evolution. These gneisses exhibit mafic inclusions of eclogitic rocks, with the thickest layer of massive eclogites (ca. 300 m) located in the basal part of the metasedimentary succession (Fig. 2). Thermobarometric determinations in these basal eclogites suggest that eclogite-facies peak conditions were reached at 750–800 °C and 20–23 kbar (real pressure; Mendiá 1996). The sample is a fine- to medium-grained porphyroblastic gneiss with a high-temperature mineral assemblage that lacks primary muscovite. The regional foliation in the gneiss formation is mylonitic and was probably developed in a post-eclogitic stage. It is defined by biotite-rich layers that alternate with quartz plagioclase-rich domains. Lepidoblastic biotite is interlocked with fibrolitic sillimanite that formed during post-eclogitic decompression. Abundant pre-schistose garnets, developed during the HP HT eclogitic event, appear as sheared porphyroblasts partially replaced by biotite. Some large crystals of rutile, partially replaced by ilmenite, and plagioclase are probably also relic mineral phases of the

eclogitic paragenesis. Locally, titanite is observed to grow synkinematically with the Variscan regional foliation.

*GCH-99-6: Chimparra Gneiss: garnet-bearing biotitic paragneiss*

The Chimparra Gneiss Formation (Vogel 1967) is formed by migmatitic paragneisses ranging in composition from pelitic to semi-pelitic (Fig. 2). Their tectono-thermal evolution is similar to that of the Banded Gneiss, but, in this case, the HP and HT event reached granulite-facies conditions, as can be deduced from the mafic inclusions within the gneisses (Vogel 1967). Sample GCH-99-6 is a migmatitic paragneiss composed of Grt Bt Pl Qtz Rt Ilm, with some retrogressive and post-schistose muscovite lepidoblasts. Medium- to fine-grained leucosomes composed of quartz and plagioclase appear flattened in the foliation, suggesting that partial melting in the Chimparra Gneiss Formation took place in early to syn-schistose stages.

*GCH-99-7. Chimparra Gneiss (Carreiro Shear Zone): Grt Ky-bearing biotitic paragneiss*

The Carreiro Shear Zone is interpreted as a Variscan thrust that placed the HP HT unit over the ophiolitic rocks representing the Variscan suture (Fig. 2). Deformation in this major thrust occurred under amphibolite-facies conditions. In the footwall to the thrust plane, metagabbroic rocks of the ophiolites were accreted and transformed into garnet amphibolites at ca. 390 Ma ( $^{40}\text{Ar}/^{39}\text{Ar}$  on hornblende concentrates; Peucat et al. 1990). In the hanging wall to the thrust plane, close to the area with the more intense deformation, the Chimparra Gneiss appears strongly mylonitised. The mineral assemblage formed during the HP and HT event has been highly overprinted, and the actual mineralogy of the paragneiss is related to the development of the mylonitic foliation. The studied sample is a porphyroblastic rock constituted by Grt Ky Bt Ms Pl Qtz Rt Ilm Czo. Porphyroblastic garnet is very common and shows late to post-tectonic relationships with the mylonitic foliation. Kyanite crystals (ca. 0.5 mm in length) are also very common and appear oriented in the foliation. Biotite is almost the only mica in the paragneiss, although some scarce muscovite lepidoblasts showing late to post-tectonic relationships with the foliation were observed.

*GCH-99-9. Leucosome in mafic granulites: Grt-bearing quartz plagioclase gneiss*

The HP mafic granulites (Fig. 2) were affected by partial melting during decompression following the HP event. During this process, the original granonematoblastic granulites (Na-Di + Grt + Pl + Qtz + Rt) were strongly deformed, melted and finally retrogressed. Thence, these mafic rocks were transformed in mafic migmatites and finally in amphibolic gneisses (Galán

and Marcos 2000). The leucosome selected for this study comes from a layer 20 cm thick. It is a very homogeneous leucocratic rock almost without mafic parts. This leucocratic gneiss exhibits a granoblastic texture and is mainly composed of alotrioblastic or sub-idioblastic crystals (<0.5 mm) of garnet, quartz and plagioclase. Other minor minerals in this gneiss are clinozoisite, green hornblende, scapolite, biotite, rutile, ilmenite and titanite. Petrographic observations show that titanite is always a late phase with respect to rutile and ilmenite.

Ordenes Complex

*GCH-99-11. Belmil Gneiss: Grt Ky-bearing biotitic paragneiss*

In the SE of the Ordenes Complex, the Belmil Antiform exhibits HP and HT paragneisses, which contain inclusions of metagabbros and mafic granulites (Fig. 3). The selected sample is a Grt Ky-bearing biotitic paragneiss that shows an important low-temperature retrogression. Most of the biotite lepidoblasts, as well as many of the kyanite (ca. 0.25–0.50 mm) and garnet crystals, have been replaced by fine-grained retrogressive aggregates with sericite, chlorite, plagioclase and clinozoisite. The groundmass in this gneiss is composed of abundant quartz and plagioclase, with scattered ilmenite crystals.

*GCH-99-13. Melide Gneiss: Grt Ky-bearing biotitic paragneiss*

To the E of the Behnil Antiform, a thin layer of HP and HT paragneisses outcrops in association with mafic and ultramafic rocks (Fig. 3). These paragneisses are located immediately below the Corredoiras Detachment, an important Variscan extensional detachment (Díaz García et al. 1999a) previously dated at 375 Ma ( $^{40}\text{Ar}/^{39}\text{Ar}$  on hornblende concentrates; Dallmeyer et al. 1997). This detachment caused an important deformation in the HP paragneisses, which appear as highly mylonitised rocks constituted by Grt Ky Bt Ms Pl Qtz Rt Ilm Czo. The mylonitic foliation is fine-grained and defined by lepidoblasts of biotite and minor muscovite, which appear interlocked with fine needles (ca. 0.1 mm) of sillimanite. Abundant porphyroclasts of quartz, plagioclase, rutile, ilmenite, garnet and kyanite are surrounded by the mylonitic foliation. The large porphyroclasts of kyanite (ca. 1 mm) belong to a first generation of this mineral and, together with the rest of the porphyroclastic minerals, can be interpreted as relics of the HP assemblage.

*GCH-99-18. Sobrado Upper Gneiss: Grt Ky-bearing biotitic paragneiss*

In the eastern part of the Ordenes Complex, the HP HT unit is exposed in the core of a tectonic window, the Sobrado Window (Fig. 3). The HP HT unit of the Sobrado Window may be subdivided into three different

slices limited by minor extensional contacts (Martinez Catalán and Arenas 1992). The lower slice is made up, from bottom to top, by highly serpentinised ultramafic rocks with some mafic inclusions and a layer of metabasites 500 m thick. These mafic rocks include eclogites (Omp + Grt + Qtz + Rt  $\pm$  Ky  $\pm$  Zo) and related clinopyroxene garnet rocks without primary plagioclase (Na-Di + Grt + Qtz + Rt  $\pm$  Zo), as well as other lithological types derived from the retrogression and mylonitization of the early high-P types. The intermediate slice contains a 1,000-m-thick package of migmatitic paragneisses (Sobrado Lower Gneiss), with frequent inclusions of HP granulite-facies mafic rocks (Na-Di + Grt + Pl + Qtz + Rt  $\pm$  Ky). Thermobarometry in these granulites suggests metamorphic peak conditions of 850 °C and 13 kbar. Relics of the igneous protoliths are not preserved either in the lower or in the intermediate slices. The upper slice includes migmatitic felsic gneisses (Sobrado Upper Gneiss) and layers of mafic rocks derived from deformed and recrystallized gabbros, which locally grade to undeformed varieties that preserve intact igneous textures. Peak conditions in these granulite-facies mafic rocks were estimated to be 750 °C and 10–11 kbar (Arenas and Martinez Catalán 1993). Later, these metabasites were affected by variable amounts of partial melting and, finally, developed a regional foliation in the amphibolite facies, whose common products include amphibolic gneisses, flaser amphibolites and fine-grained amphibolites. The partial melting process and the later mylonitization also affected the metabasites of the intermediate slice, as well as the paragneisses. Sample GCH-99-18 is a migmatitic paragneiss that shows an important low-temperature retrogression. Most of the garnet porphyroblasts, kyanite crystals and biotite lepidoblasts have been replaced by mineral aggregates with chlorite and muscovite. The groundmass in this gneiss is mainly constituted by quartz and plagioclase with minor ilmenite crystals developed after rutile.

*GCH-99-17. Sobrado Lower Gneiss:  
Grt Ky Kfs-bearing migmatitic paragneiss*

This is a medium-grained, biotite-poor granoporphyroblastic gneiss. Large porphyroblasts of garnet and kyanite (up to 1 mm) are surrounded by an intense, mylonitic foliation. Some pre-schistose rutile grains are partially replaced by ilmenite. The scarce lepidoblasts of biotite oriented in the foliation are frequently developed by a reaction that involves garnet breakdown. Therefore, it can be suggested that in the Sobrado Window, as was also the case in the HP and HT paragneisses of the Cabo Ortegal Complex, the regional mylonitic foliation in the HP HT paragneisses is younger than the HP event. In some cases, especially in the proximity of major Variscan structures, the early mylonitic foliation was reactivated during Variscan times. Thus, it can be suggested that this foliation has a polymetamorphic development. Partial melting occurring during the first stages

of development of the mylonitic foliation is well documented in this paragneiss, where Qtz Pl Kfs syn-schistose leucosomes are widespread.

## U–Pb dating

### Analytical techniques

U–Pb analytical work was conducted at the Mineralogical Geological Museum, University of Oslo. Samples were crushed with a jaw crusher and pulverised with a hammer mill. Minerals were separated by heavy fraction enrichment on a Wilfley table, magnetic separation in a Frantz isodynamic separator and density separation using di-iodomethane (CH<sub>2</sub>I<sub>2</sub>). Minerals to be analysed were hand picked under a binocular microscope and some of the fractions were subsequently air-abraded (see Table 1) following the method of Krogh (1982). The selected minerals were washed in 4 N HNO<sub>3</sub> on a hotplate and rinsed repeatedly with H<sub>2</sub>O and acetone. A mixed <sup>205</sup>Pb/<sup>235</sup>U spike was added to the sample after weighing and transfer to the dissolution vessel. Zircon and rutile were dissolved in HF (+ HNO<sub>3</sub>) in Teflon minibombs at ca. 185 °C, monazite was dissolved in 6 N HCl in Savillex vials on a hotplate and titanite was dissolved in HF (+ HNO<sub>3</sub>) using Savillex vials on a hotplate. The solutions were subsequently evaporated, redissolved in 3.1 N HCl and passed through anion exchange columns in HCl medium to purify U and Pb (zircon and monazite). For titanite and rutile, a procedure using HCl–HBr–HNO<sub>3</sub> was used (Corfu and Stott 1986). Pb and U were finally collected together in the bombs/Savillex vials used for dissolution and loaded together on outgassed Re filaments with H<sub>3</sub>PO<sub>4</sub> and silica gel. Isotopic ratios were measured on a Finnigan-MAT 262 mass spectrometer using up to four Faraday detectors in multicollection mode. Very small fractions or fractions with very small amounts of U and Pb were measured by peak jumping on a secondary electron multiplier (ion counting mode). Total procedural blanks were less than 2–5 pg Pb and 0.1–0.3 pg U for zircon and monazite, and 10 pg Pb and 0.3 pg U for titanite and rutile. The Stacey and Kramers (1975) model was used to subtract initial common Pb in excess of the laboratory blank. Regression lines were calculated using the model 1 algorithm of Ludwig (1989) with intercept errors quoted at 95% confidence level. Decay constants are those of Jaffey et al. (1971).

## Results

A total of 23 monazite, 14 zircon, four titanite and one rutile analyses were performed on single and multigrain fractions. The results are given in Table 1 and in the concordia plots of Figs. 4, 5, 6, 7, 8 and 9. The general features of analytical data and the results are reported below.



Table 1. Results of U–Pb dating

Sample, analysis, mineral <sup>a</sup> features	Weight <sup>b</sup> (mg)	U (ppm)	Th/U <sup>c</sup>	Total Pb in sample <sup>d</sup> (pg)	<sup>206</sup> Pb <sup>e</sup>	<sup>206</sup> Pb <sup>f</sup>	$2\sigma$ <sup>g</sup>	<sup>207</sup> Pb	$2\sigma$	<sup>207</sup> Pb	$2\sigma$	Apparent age (Ma)		
					<sup>238</sup> U	<sup>235</sup> U	(absolute)	<sup>235</sup> U	(absolute)	<sup>206</sup> Pb	<sup>207</sup> Pb	<sup>207</sup> Pb		
Cabo Ortegal Complex														
GCH-99-1														
z, sb, <b>eq</b> , A (14)	18	147	0.13	17.6	1,065	0.11108	0.00027	1.3244	0.0051	0.08648	0.00022	679.0	856.4	1,348.8
z, sb, lp, A (9)	12	412	0.13	2.7	5,269	0.09044	0.00023	0.8736	0.0028	0.07006	0.00012	558.1	637.5	930.1
z, <b>eq</b> , sb (multifacet) A (15)	15	230	0.31	11.9	3,652	0.19940	0.00039	3.0912	0.0067	0.11243	0.00009	1,172.1	1,430.5	1,839.1
z, eu, lp (needles), A (15)	12	76	0.35	3.4	2,729	0.07654	0.00027	0.5986	0.0023	0.05672	0.00016	475.4	476.4	480.8
m, sb, <b>eq</b> , nA (1)	1	2,800	15.43	3.1	3,532	0.06196	0.00017	0.4620	0.0016	0.05408	0.00013	387.5	385.6	374.4
m, sb, <b>eq</b> , nA (1)	1	696	64.06	2.8	1,075	0.06796	0.00025	0.5223	0.0035	0.05574	0.00032	423.9	426.7	441.9
m, sb, <b>eq</b> (turbid), nA (1)	4	667	43.39	73.8	165	0.06495	0.00092	0.4866	0.0291	0.05433	0.00304	405.7	402.6	384.9
t, sb, pg, incl, A (>50)	300	13	1.20	1,526.8	29	0.06439	0.00218	0.5127	0.1330	0.05775	0.01510	402.3	420.3	520.2
t, sb, pg, incl, A (>50)	550	21	0.61	4,074.0	30	0.06468	0.00203	0.5852	0.1251	0.06562	0.01415	404.0	467.8	794.2
GCH-99-6														
m, sb-an, <b>eq</b> , nA (10)	19	1,725	3.52	11.0	14,312	0.07654	0.00019	0.5994	0.0015	0.05680	0.00007	475.4	476.9	483.9
GCH-99-7														
m, sb, <b>eq</b> , nA (16)	30	1,426	3.46	23.5	8,249	0.07208	0.00040	0.5560	0.0028	0.05595	0.00015	448.7	448.9	450.2
m, sb, <b>eq</b> , nA (14)	30	2,768	4.56	25.0	15,025	0.07203	0.00019	0.5564	0.0015	0.05602	0.00003	448.3	449.2	453.3
m, sb, <b>eq</b> , A (1)	2	2,656	2.76	4.2	18,536	0.07822	0.00025	0.6144	0.0022	0.05696	0.00008	485.5	486.3	490.2
m, sb, <b>eq</b> , A (1)	2	2,490	5.34	9.6	2,522	0.07743	0.00018	0.6045	0.0020	0.05662	0.00010	480.8	480.1	476.8
m, sb, <b>eq</b> , nA (1)	1	662	4.37	4.9	3,979	0.07338	0.00024	0.5678	0.0022	0.05612	0.00009	456.5	456.6	457.0
m, sb, <b>eq</b> , nA (1)	2	192	4.32	2.3	4,900	0.07503	0.00029	0.5825	0.0024	0.05630	0.00014	466.4	466.1	464.3
GCH-99-9														
z, eu, f, <b>eq</b> , A (5)	10	13	0.07	12.9	62	0.07100	0.00062	0.5288	0.0631	0.05402	0.00615	442.2	431.0	371.9
z, eu, <b>eq</b> (multifacet) A (5)	8	11	0.08	1.5	279	0.06881	0.00039	0.5307	0.0139	0.05593	0.00136	429.0	432.3	449.7
z, eu, lp, A (6)	5	67	0.13	11.9	161	0.08101	0.00043	0.6896	0.0130	0.06174	0.00111	502.1	532.6	665.2
z, eu, lp (stubby), A (25)	250	113	0.10	8.0	17,233	0.07802	0.00044	0.6133	0.0034	0.05701	0.00008	484.3	485.6	491.8
z, eu, lp, A (25)	198	122	0.10	11.4	10,457	0.07833	0.00068	0.6141	0.0053	0.05686	0.00007	486.2	486.2	486.1
z, sb, tips, A (30)	128	120	0.09	13.1	5,704	0.07751	0.00030	0.6099	0.0025	0.05707	0.00011	481.2	483.5	494.3
t, sb, pg, A (>50)	670	18	0.11	1283.8	53	0.06173	0.00065	0.4652	0.0387	0.05466	0.00456	386.2	387.9	398.2
t, sb, pg, A (>50)	610	15	0.21	949.2	56	0.06205	0.00061	0.4680	0.0367	0.05471	0.00430	388.1	389.8	400.4
rt, sb, A (>50)	240	18	0.04	43.6	54	0.05940	0.00060	0.4113	0.0369	0.05022	0.00449	372.0	349.8	205.0
Ordenes Complex														
GCH-99-11														
m, sb, <b>eq</b> , nA (10)	20	4,384	6.55	71.8	5,411	0.07046	0.00054	0.5472	0.0042	0.05632	0.00013	438.9	443.1	465.2
m, sb, <b>eq</b> , A (4)	10	1,065	4.91	3.3	15,853	0.07879	0.00018	0.6203	0.0017	0.05710	0.00008	488.9	490.0	495.3
m, sb, <b>eq</b> , A (6)	13	2,032	6.25	8.4	15,800	0.07964	0.00023	0.6283	0.0019	0.05722	0.00005	494.0	495.0	500.0
m, sb, <b>eq</b> , A (1)	1	240	3.05	3.3	2,561	0.07926	0.00024	0.6220	0.0024	0.05692	0.00013	491.7	491.1	488.3
m, sb, <b>eq</b> , A (1)	1	244	3.45	2.0	4,067	0.07940	0.00024	0.6244	0.0024	0.05703	0.00013	492.5	492.6	492.9
GCH-99-13														
m, sb, <b>eq</b> , nA (20)	49	603	19.11	20.4	5,629	0.06180	0.00012	0.4626	0.0010	0.05429	0.00005	386.6	386.1	383.1
m, sb, <b>eq</b> , A (18)	47	882	17.35	32.7	4,912	0.06162	0.00028	0.4599	0.0022	0.05413	0.00007	385.4	384.2	376.6
m, sb, <b>eq</b> , A (20)	43	882	17.45	34.7	4,668	0.06207	0.00038	0.4635	0.0029	0.05416	0.00012	388.2	386.7	377.5
m, sb, <b>eq</b> , A (1)	1	641	29.05	1.2	3,871	0.06213	0.00021	0.4657	0.0019	0.05436	0.00014	388.5	388.2	386.2
m, sb, <b>eq</b> , A (1)	1	75	25.00	2.0	320	0.06163	0.00027	0.4622	0.0105	0.05440	0.00116	385.5	385.8	387.6
GCH-99-18														
m, sb, <b>eq</b> , A (5)	12	877	4.65	12.5	24,083	0.07905	0.00024	0.6203	0.0017	0.05691	0.00009	490.4	490.0	488.0
m, sb, <b>eq</b> , A (1)	1	1,441	3.44	5.9	8,206	0.07867	0.00029	0.6170	0.0025	0.05689	0.00009	488.2	488.0	487.2
m, sb, <b>eq</b> , A (1)	2	1,118	3.30	3.9	19,387	0.07751	0.00031	0.6080	0.0027	0.05689	0.00006	481.2	482.3	487.3
GCH-99-17														
z, eu, stubby, A (1)	25	57	0.21	2.1	10,365	0.17048	0.00056	2.5579	0.0091	0.10882	0.00018	1,014.7	1,288.7	1,779.8
z, eu, <b>eq</b> , f, A (25)	37	185	0.16	9.5	40,232	0.10745	0.00072	1.2760	0.0087	0.08613	0.00006	657.9	835.1	1,341.0
z, eu, <b>eq</b> , f, A (5)	13	352	0.22	4.7	5,805	0.13613	0.00032	1.9089	0.0046	0.10170	0.00010	822.7	1,084.2	1,655.4
z, eu, lp, (tiny incl), A (30)	116	199	0.24	11.5	25,823	0.20508	0.00061	3.6556	0.0113	0.12928	0.00007	1,202.6	1,561.7	2,088.2

<sup>a</sup>m Monazite; z zircon; t titanite; rt rutile; eu euhedral; sb subhedral; an anhydral; eq equant; lp long prisms; f flat; pg pale green; A abraded; nA not abraded; (1) number of grains analysed

<sup>b</sup>Weights better than 10% when sample weight is over 10 mg

<sup>c</sup>Model Th/U ratio estimated from <sup>203</sup>Pb/<sup>206</sup>Pb ratio and age of the sample

<sup>d</sup>Total common Pb in sample, including initial and blank Pb

<sup>e</sup>Measured ratio, corrected for fractionation and spike contribution  
<sup>f</sup>Corrected for spike, fractionation, blank and initial common Pb (Stacey and Kramers 1975)

<sup>g</sup> $2\sigma$  uncertainty calculated by error propagation procedure that takes into account internal measurement statistics and external reproducibility as well as uncertainties in blank and common Pb correction

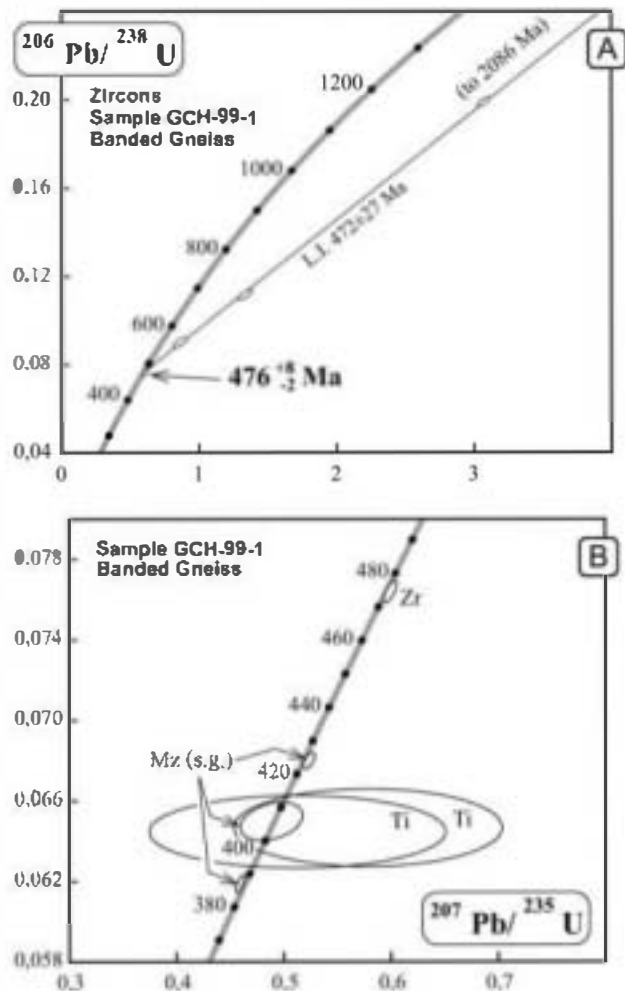


Fig. 4. U-Pb concordia diagram showing the results of A U-Pb dating of zircon and B monazite and titanite from eclogite-facies paragneiss GCH-99-1 (Banded Gneiss). Errors are given at the  $2\sigma$  level. s.g. Single grain analysis in this figure and Figs. 5, 6, 7, 8 and 9

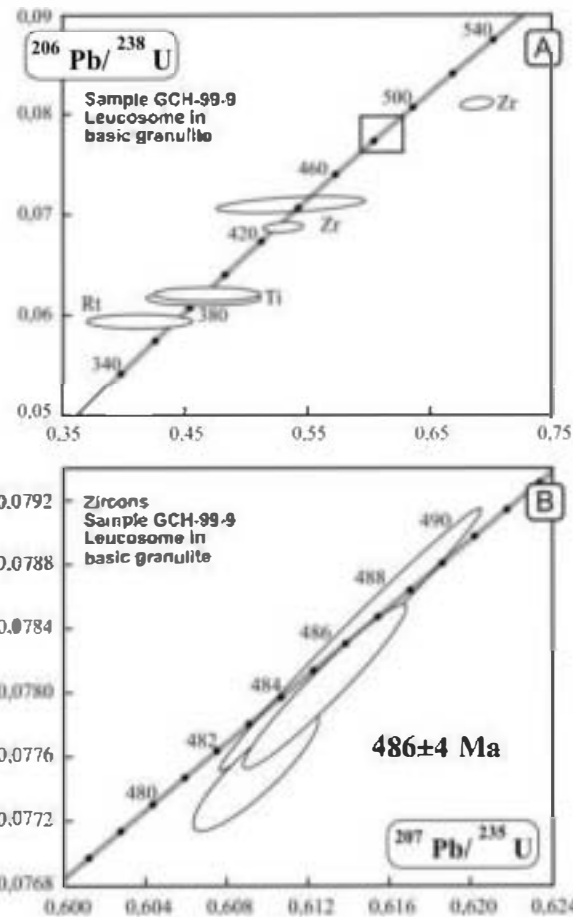


Fig. 6. U-Pb concordia diagram showing the results of U-Pb dating of A zircon, titanite and rutile and B zircon (enlargement of box in A) from leucosome GCH-99-9 in mafic granulites. Errors are given at the  $2\sigma$  level

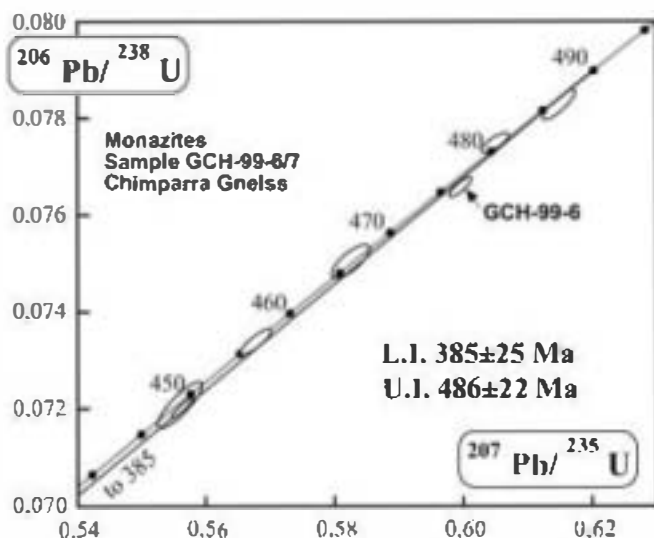


Fig. 5. U-Pb concordia diagram showing the results of U-Pb dating of monazite from paragneiss samples GCH-99-6 and -7 (Chimparra Gneiss). Errors are given at the  $2\sigma$  level

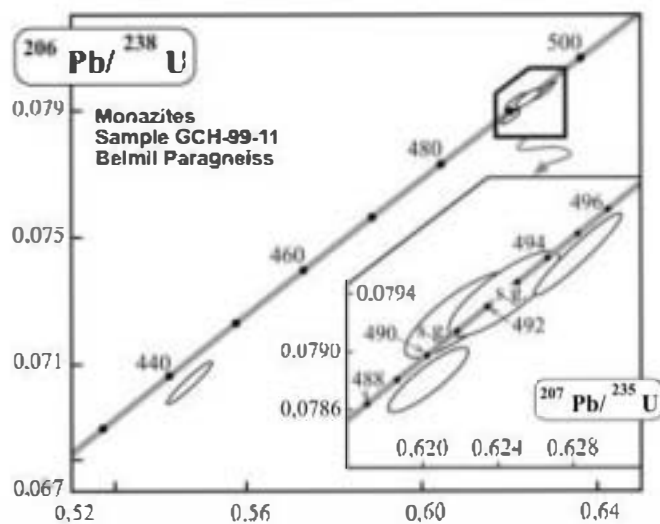


Fig. 7. U-Pb concordia diagram showing the results of U-Pb dating of monazite from paragneiss sample GCH-99-11 (Belmil Gneiss). Errors are given at the  $2\sigma$  level

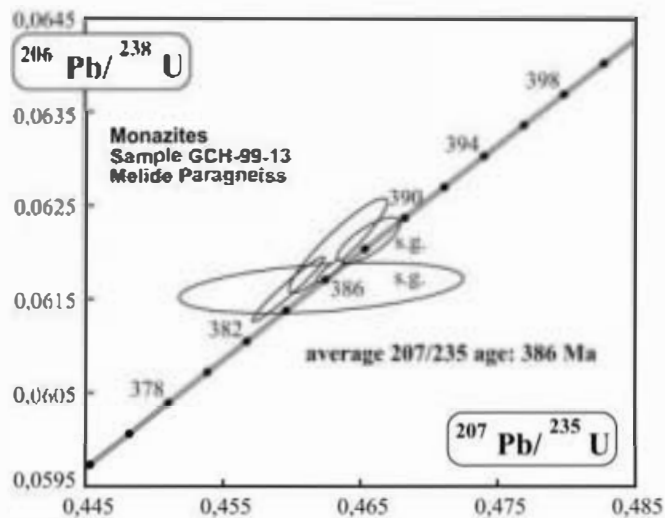


Fig. 8. U-Pb concordia diagram showing the results of U-Pb dating of monazite from paragneiss sample GCH-99-13 (Melide Gneiss). Errors are given at the  $2\sigma$  level

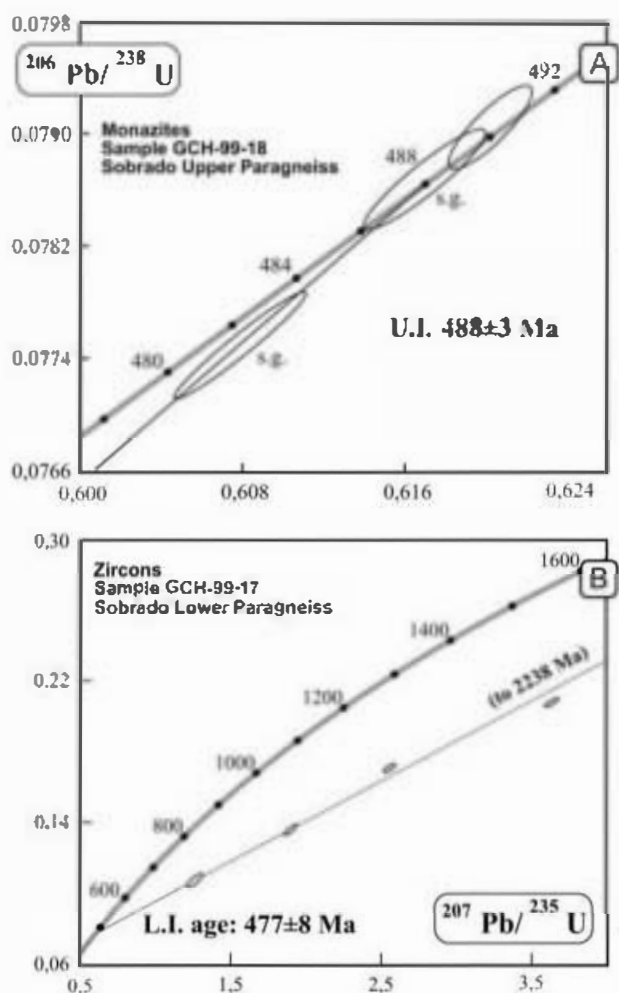


Fig. 9. U-Pb concordia diagram showing the results of U-Pb dating of A monazite in sample GCH-99-18 (Sobrado Upper Gneiss) and B zircon in sample GCH-99-17 (Sobrado Lower Gneiss). Errors are given at the  $2\sigma$  level

### Banded Gneiss (GCH-99-1)

This sample contained very altered, soft, inclusion-rich monazite that either disintegrated after ca. 15 min (Fig. 4) of air abrasion or dissolved partly in a hot  $\text{HNO}_3$  bath. These grains, therefore, were considered unsuitable for analysis. Only three monazite grains of better quality and free of inclusions were found and subsequently analysed as single-grain (non-abraded) fractions. One yielded a precise analysis plotting slightly above concordia (reverse discordance, Schärer 1984; Parrish 1990) with a  $^{207}\text{Pb}/^{235}\text{U}$  age of 386 Ma. A second single grain yielded a normally discordant point with a  $^{207}\text{Pb}/^{206}\text{Pb}$  age of  $442 \pm 13$  Ma. A third, lower quality single grain yielded an imprecise analysis (possibly owing to alteration-related anomalous monazite composition affecting separation of U and Pb) with a  $^{207}\text{Pb}/^{235}\text{U}$  age of 402.6 Ma (and a  $^{207}\text{Pb}/^{206}\text{Pb}$  age of  $385 \pm 22$  Ma, Table 1). Two fractions of titanite were analysed. Both contained abundant inclusions and even intense air abrasion could not eliminate many of the opaque inclusions. The two analyses have low precision, but overlap with one another yielding a mean  $^{206}\text{Pb}/^{238}\text{U}$  age of ca. 403 Ma. This sample contained abundant zircons. Four small multi-grain fractions were analysed. Three of the fractions are discordant reflecting Precambrian inherited components. A fourth fraction of very small needle-like prisms yielded a subconcordant point (1.2% discordia) with a  $^{207}\text{Pb}/^{206}\text{Pb}$  age of 480.8 Ma. The four fractions lie along a discordia line with a lower intercept at  $472 \pm 27$  Ma.

### Chimparra Gneiss (GCH-99-6,7)

Two samples of the Chimparra Gneiss were investigated (Fig. 5). The first sample (6) contained very little monazite and only one small multigrain fraction analysis was performed, yielding a slightly normally discordant point (1.8% discordance) with a  $^{207}\text{Pb}/^{206}\text{Pb}$  age of 484 Ma. The second sample, collected within the Variscan Carreiro Shear Zone contained abundant monazite and six analyses (four single and two multigrain fractions) were performed. The two non-abraded multigrain fractions yielded overlapping data points with a mean  $^{207}\text{Pb}/^{235}\text{U}$  age of 449 Ma, although the more precise analysis is 1.1% discordant with a  $^{207}\text{Pb}/^{206}\text{Pb}$  age of 453 Ma. The single grain (abraded) fractions yielded concordant (0.5 to 1% discordance) ages ranging from 457 to 486 Ma ( $^{207}\text{Pb}/^{235}\text{U}$  ages; Fig. 5).

### Leucosome in mafic granulites (GCH-99-9)

Six zircon, two titanite and one rutile abraded fractions were analysed (Fig. 6). Two of the zircon fractions were very low in uranium ( $< 13$  ppm) resulting in analyses with large  $^{207}\text{Pb}/^{235}\text{U}$  and  $^{207}\text{Pb}/^{206}\text{Pb}$  uncertainties. The  $^{206}\text{Pb}/^{238}\text{U}$  ages are  $442 \pm 4$  (small short flat euhedral prisms) and  $429 \pm 3$  Ma (equant multifaceted 'football-like' zircons). One fraction of long euhedral prisms

contained an inherited component yielding a  $^{207}\text{Pb}/^{206}\text{Pb}$  age of 665 Ma. One large fraction of more U-rich, big euhedral stubby prisms yielded a subconcordant (1.6% discordance) point with a U/Pb age of  $485 \pm 3$  Ma and a  $^{207}\text{Pb}/^{206}\text{Pb}$  age of  $492 \pm 4$  Ma. One fraction of zircon was similar in morphology to the previous fraction, but was smaller in size and yielded a concordant age of  $486 \pm 4$  Ma. A third fraction of tips of large prisms yielded a slightly discordant data point with a  $^{207}\text{Pb}/^{206}\text{Pb}$  age of  $494 \pm 4$  Ma. The two titanite fractions yielded overlapping data points with a mean  $^{206}\text{Pb}/^{238}\text{U}$  age of 387 Ma. The rutile fraction yielded a  $^{206}\text{Pb}/^{238}\text{U}$  age of 372 Ma.

#### Belmil Gneiss (GCH-99-11)

Five monazite fractions (two single grain and three multigrain) were analysed (Fig. 7). The largest fraction was not abraded and yielded a discordant point with a  $^{207}\text{Pb}/^{206}\text{Pb}$  age of 465 Ma. The two single grain fractions are concordant and yielded overlapping data points with a mean  $^{207}\text{Pb}/^{235}\text{U}$  age of 492 Ma. The two abraded multigrain fractions are slightly discordant (1.2 and 1.3% discordant) with  $^{207}\text{Pb}/^{206}\text{Pb}$  ages of 495 and 500 Ma.

#### Melide Gneiss (GCH-99-13)

Five monazite fractions (two abraded single grains, one non-abraded and two abraded multigrain fractions) were analysed (Fig. 8). All data cluster tightly on or slightly above concordia with  $^{207}\text{Pb}/^{235}\text{U}$  ages in the range 384–388 Ma. As shown in Fig. 8, no evidence was found for any older stage of monazite growth.

#### Sobrado Upper Gneiss (GCH-99-18)

Three abraded monazite fractions (two single grains and one multigrain) were analysed (Fig. 9a). The multigrain fraction and one single grain yielded overlapping concordant data points with an average  $^{207}\text{Pb}/^{235}\text{U}$  age of 489 Ma. The second single grain analysis is slightly discordant and yielded a  $^{207}\text{Pb}/^{206}\text{Pb}$  age of 487 Ma (within error of the U/Pb age of the concordant data). These ages are in agreement with that obtained by Kuijper (1979) in a monazite multigrain fraction separated from a sample of the same unit in a different locality ( $^{207}\text{Pb}/^{206}\text{Pb}$  age 487 Ma).

#### Sobrado Lower Gneiss (GCH-99-17)

This quartz feldspathic migmatitic paragneiss did not contain monazite (Fig. 9b). Three multigrain zircon fractions and one single grain (all abraded) were analysed. The four fractions are discordant and contain Precambrian inherited components. Although the four fractions do not fit on a regression line, a discordia line through the two fractions with the lowest

$^{207}\text{Pb}/^{206}\text{Pb}$  ages gives a lower intercept age of  $477 \pm 8$  Ma, which is in agreement with that obtained by Kuijper (1979) in the paragneisses of the lower unit ( $472 \pm 12$  Ma). This age is also consistent with the subconcordant fraction of sample GCH-99-1 ( $^{207}\text{Pb}/^{206}\text{Pb}$  age 481 Ma).

### Discussion of U–Pb results

The results presented in the previous section are further discussed in this section. All samples except the leucosome (GCH-99-9) correspond to eclogite- to granulite-facies paragneisses, which, in some cases, show evidence of melting (see sample description above). A prominent feature evidenced by the data set is that there is no apparent difference between the Ordenes and Cabo Ortegal results and, therefore, they will be considered together in the following discussion (this is also consistent with the geological evolution of the AC, see above).

#### Zircon data

Interpretation of zircon U/Pb data in metamorphic rocks is often complex (see review in Mezger and Krogstad 1997). In the present study, we dated zircons from a leucosome in order to constrain its crystallisation age and zircons from an eclogite-facies paragneiss (GCH-99-1) and from a granulite-facies paragneiss (GCH-99-17). Both paragneisses show clear field evidence of migmatization, which is interpreted to have occurred during decompression following peak pressure conditions.

In the case of the leucosome (Fig. 6), the crystallisation age is well constrained by one concordant fraction of euhedral prisms, and two slightly discordant fractions whose  $^{207}\text{Pb}/^{206}\text{Pb}$  ages overlap within error with that of the concordant fraction (Table 1, Fig. 6). The crystallisation age is best constrained as  $486 \pm 4$  Ma, also considering that the two slightly discordant fractions may be displaced to the right owing to some minor inheritance. The fraction with a Precambrian component reflects inheritance in the protolith (mafic granulite derived from a gabbro), whose crystallisation age is thought to be only slightly older than that of the high-grade metamorphic event (Peucat et al. 1990; Ordóñez Casado 1998). The low-U fractions, although yielding imprecise analyses, reflect the presence of a younger component. Based on the more precise  $^{206}\text{Pb}/^{238}\text{U}$  ages (ca. 430–440 Ma) they lie between the older concordant age and the younger ages recorded by titanite and rutile (see below and Fig. 6). The very low U content of these zircons (Table 1) suggests that lead-loss is not likely to have caused a shift towards younger ages. Given that there is no independent evidence for a geological event at 430–440 Ma, the most likely explanation is that these fractions represent a mixture of 486-Ma cores and

overgrowths related to a later event as recorded by titanite growth. It should also be noted that these zircons are very different in morphology from those belonging to the 486-Ma generation.

Eclogite facies paragneiss (GCH-99-1, Fig. 4) contained abundant zircons of assorted morphology and size (Table 1). The subconcordant fraction with a  $^{207}\text{Pb}/^{206}\text{Pb}$  age of 481 Ma was formed by very small needle-like transparent euhedral prisms. Considering that the protolith must have been a pelitic to semipelitic sediment, this datum, taken at face value, could be explained in two ways: (1) these zircons represent  $\geq 481$  Ma detrital components that only suffered slight Pb loss throughout subsequent events, or (2) they are new zircons grown metamorphically or in small melt pools within the paragneiss. It should be noted that these very carefully selected 15 crystals were practically identical to one another and that they represent a distinct morphological type within the zircon population of the sample. Because monazite data indicate that the HP HT units underwent high-grade metamorphism at an age older than ca. 481 Ma, the first possibility must be ruled out. This is also in agreement with the significantly older depositional ages proposed for these metasediments (Ordóñez Casado 1998). The three discordant fractions represent the main morphological types found in the sample (multifaceted equant crystals, equant subhedral to euhedral transparent prisms and long subhedral prisms). The fraction with the oldest apparent age is that formed by the equant football-like crystals. The others yield much younger  $^{207}\text{Pb}/^{206}\text{Pb}$  ages (Table 1), suggesting that they might be formed by grains with old cores and overgrowths coeval with the sub-concordant fraction. This is supported by the regression shown in Fig. 4a, which yields a lower intercept age of  $472 \pm 27$  Ma, within error of the subconcordant fraction. Furthermore, a regression not constrained by the subconcordant fraction (i.e. using only the three discordant fractions) yields a lower intercept age of 470 Ma, although the probability of fit is 0. In this case we consider that the lower intercept is meaningful (cf. Discussion in Mezger and Krogstad 1997) and represents an event at ca. 470–480 Ma or slightly older. The argument is strengthened by the presence of the sub-concordant fraction at the end of the discordia chord. Although there is a 20% probability that this age is concordant with a concordia age of  $476 \pm 1.5$  Ma (Ludwig 1998), it is possible that these needles may have been affected by minor lead-loss. As a more prudent estimate, zircon is constrained as  $476 \pm 8/2$  Ma.

The migmatitic (granulite-facies) paragneiss GCH-99-17 also contained abundant zircons. The four fractions are discordant with  $^{207}\text{Pb}/^{206}\text{Pb}$  ages ranging from ca. 1.3 to 2.09 Ga and on a concordia plot show the typical array of zircons from high-grade metamorphic rocks (Fig. 9b). The single large euhedral prism yielded a  $^{207}\text{Pb}/^{206}\text{Pb}$  age of 1.77 Ga, similar to a multigrain fraction with a  $^{207}\text{Pb}/^{206}\text{Pb}$  age of 1.65 Ga. The latter consisted of small equant euhedral prisms included in

biotite (separated from biotite flakes in the magnetic fraction). A regression using only the two fractions with the smallest proportion of inherited Pb (both very similar in morphology, consisting of small flat euhedral prisms) yields a lower intercept age of  $477 \pm 8$  Ma (Fig. 9b); the two other fractions lie close to the line, one at each side. Because of the low U content, the zircons from this rock would not have undergone much Pb loss after the 477 Ma event. Given that (1) the lower intercept of ca. 477 Ma is consistent with the lower intercept (plus concordant fraction) in the previous sample ( $472 \pm 27$  Ma), and (2) it is consistent with the lower intercept age obtained by Kuijper (1979) in a similar sample from the same unit ( $472 \pm 12$  Ma), we consider the lower intercept to be significant and evidence for a high-grade geological event at ca. 470–480 Ma.

The consistency of data between the eclogite facies paragneiss (Cabo Ortegal Complex, Fig. 2) and the granulite-facies paragneiss (Ordenes Complex; Fig. 3) also support our hypothesis that these ages are meaningful and represent an event affecting the HP HT units of the Allochthonous Complexes at ca. 470–480 Ma. Finally, these ages are consistent (within analytical error) with the crystallisation age of the leucosome and suggest that the event responsible for melting in the mafic granulites was coeval with the growth of new zircon in the HP HT paragneisses.

The upper intercept age in the granulite facies migmatitic paragneiss (Fig. 9b) is ca. 2.2 Ga, indicating that the average age of the inherited component is very similar in the metasediments of the two AC investigated (cf. Figs. 4a and 9b), which, in turn, is consistent with geological observations suggesting that the HP HT units have a common geological evolution in all the AC of NW Iberia and that, in particular, the sedimentary protoliths of the HP HT gneisses were formed in the same environment and, therefore, carried the same admixture of detrital zircons. These new data are also in agreement with those of Peucat et al. (1990) for rocks of the same units and with SHRIMP data (Ordóñez Casado 1998), which point to a predominance of Early Proterozoic detrital zircons in these HP HT paragneisses.

### Monazite data

All samples except the leucosome (GCH-99-9) and the migmatitic paragneiss (GCH-99-17) contained monazite. It is well known that monazite is a suitable mineral for isotopic monitoring of high-grade events owing to its resilience to lead loss, its high closure temperature and the general absence of inherited components. In addition, monazite U–Pb chronology can provide information on the prograde path of a metamorphic rock. However, many studies have shown that monazite ages are often not straightforwardly interpretable and even single grains may record complex isotopic histories (e.g. Parrish 1990; Hawkins and Bowring 1997; Crowley and Ghent 1999; Vavra and Schaltegger 1999; Zhu and



O'Nions 1999; Simpson et al. 2000). The growth of monazite during the course of amphibolite granulite eclogite facies prograde metamorphism is widely documented (see references above). The rather complex history of the sample suite selected for this study is reflected in the variety and lack of uniformity of the data. Two main patterns were found: one where all data cluster in a narrow age interval and the other where the ages are spread over a larger period of time. Within the first group we have samples GCH-99-13 and -18, which themselves represent two extreme cases: in sample 13 all multi-grain and single grain fractions (abraded and non-abraded) yield Early Devonian ages (390–385 Ma) whereas in sample 18 a multigrain and two single grain fractions give Early Ordovician ages (486–490 Ma).

Sample 6 (biotite-poor quartz feldspathic paragneiss) contained very little monazite and only one small multigrain fraction was analysed (see above) yielding a slightly discordant point that reflects minor lead loss from an Early Ordovician age (Fig. 5).

Samples GCH-99-1, -7 and -11 display a spread of ages with different features in each case. In sample GCH-99-1 only three single grains were analysed (see above) to yield different ages. One datum is precise and yields a reversely discordant analysis (Table 1) with a  $^{207}\text{Pb}/^{235}\text{U}$  age of ca. 386 Ma (in the same range as the cluster of sample 13). The second grain yielded an imprecise analysis with an older  $^{207}\text{Pb}/^{235}\text{U}$  age that overlaps with the  $^{206}\text{Pb}/^{238}\text{U}$  age of two titanite fractions from the same sample (see below). The third single grain yields a 4.2% discordant analysis with a  $^{207}\text{Pb}/^{206}\text{Pb}$  age of 442 Ma. The reverse discordance (3.6%) in the first single grain is indicative of growth rather than resetting of older monazite because the excess  $^{230}\text{Th}$  could only have been incorporated during crystallisation (e.g. Parrish 1990; Vavra and Schaltegger 1999; Simpson et al. 2000). The uppermost monazite data point may represent either incomplete episodic Pb loss, or a binary mixing between Ordovician monazite (grown during the high grade event recorded by zircon in the same rock) and Devonian monazite (as the other two single grains), or a combination of both. There is no independent evidence for any event at ca. 440 Ma in any of the rocks studied except for the low U zircons in the leucosome sample that fall broadly in the same age range. Therefore, the possibility exists that something significant occurred at ca. 430–440 Ma. No concordant monazites were found matching the age of the concordant zircon fraction (see above). However, it is important to note that, with the exception of the three grains analysed, all the monazites were turbid, inclusion ridden and altered, and could not be analysed. We favour the idea that the two highest quality monazite grains with Devonian age could have formed as a result of localised fluid infiltration.

Sample GCH-99-7 belongs to the same unit as sample 6 (Fig. 3), but was collected within a Variscan amphibolite facies shear zone. Here, the situation is more complex as can be seen in Fig. 5 and Table 1. Two non-

abraded multigrain fractions yielded overlapping data points with  $^{207}\text{Pb}/^{235}\text{U}$  ages of 448.9 and 449.2 Ma. The rest of the fractions were all single grains, of which two were abraded and two non-abraded. The four analyses are sub-concordant (Fig. 5) and the  $^{207}\text{Pb}/^{235}\text{U}$  ages spread from 456 to 486 Ma, but the youngest ages were obtained from the two non-abraded grains and the oldest ones from the abraded grains. The oldest grain (1% normally discordant) has a  $^{207}\text{Pb}/^{206}\text{Pb}$  age of 490 Ma, whereas the second oldest is 0.9% reversely discordant and has a  $^{207}\text{Pb}/^{235}\text{U}$  age of 480.1 Ma. Keeping in mind the monazite age obtained in the multigrain fraction from sample 6 ( $^{207}\text{Pb}/^{206}\text{Pb}$  age 484 Ma) we believe that these two grains might reflect the Early Ordovician event in the Chimparra Gneiss unit at 480–490 Ma. The younger ages define a sub-concordant linear array that strongly suggests the presence of binary mixing in the single grains. It is very important to note that all four younger analyses correspond to non-abraded single and multigrain fractions. A simple explanation that would account for the pattern observed in this sample is that monazites occur as composite grains with an old core (480–490 million years old) and a younger overgrowth, which in the case of the older grains was totally or almost totally removed by air abrasion (e.g. Crowley and Ghent 1999). The age of the young end member component is probably 385–390 Ma, as we found in samples 13 and 1. The mixing is illustrated in Fig. 5 by the discordia line anchored at 385 Ma and calculated using all fractions. As can be seen in the figure, in this region of concordia, all younger fractions could be apparently concordant and still lie on a discordia line with an upper intercept age of ca. 486 Ma.

Sample GCH-99-11 (Fig. 7) also yielded a normally discordant analysis with a  $^{207}\text{Pb}/^{206}\text{Pb}$  age of 465 Ma for a non-abraded multigrain fraction. In this case, the source of the discordancy is hard to constrain. As proposed for previous cases, it could be a mixture of old (ca. 490 Ma) and younger (380–390 Ma by analogy with other samples) monazite. However, a discordia line anchored at 492 Ma gives a lower intercept age of ca. 275 Ma (not shown), which does not agree with such a binary mixing. An alternative could be that discordancy is caused by incomplete Pb loss (accompanied or not by new monazite growth) during a late-Variscan thermal event (cf. Dallmeyer et al. 1997). However, the presence of some Early Devonian component cannot be entirely ruled out. The rest of the fractions consisting of abraded grains yielded ages in the range 490–500 Ma. The two concordant, overlapping fractions correspond to very small, subhedral shiny single grains, whereas the two discordant fractions correspond to large brownish, U-rich grains (Table 1). These data suggest that the duration of the Early Ordovician event in this unit was of about 9 Ma from ca. 500 Ma ( $^{207}\text{Pb}/^{206}\text{Pb}$  age of the oldest discordant single grain) down to ca. 491 Ma ( $^{207}\text{Pb}/^{235}\text{U}$  age of the youngest concordant grain).

Only four titanite and one rutile fractions were analysed in the leucosome (GCH-99-9; Fig. 6a) and in the eclogite-facies paragneiss (sample GCH-99-1; Fig. 4b). Titanite and rutile are characterised by low U and Pb abundances compromising the precision of  $^{207}\text{Pb}/^{235}\text{U}$  and  $^{207}\text{Pb}/^{206}\text{Pb}$  ages through the common lead correction. Therefore, the  $^{206}\text{Pb}/^{238}\text{U}$  ages are considered for these two minerals. In the leucosome sample (Fig. 6a), two abraded fractions of pale greenish titanite yielded overlapping data points with  $^{206}\text{Pb}/^{238}\text{U}$  ages of 386 and 388 Ma. Because titanite growth in this leucosome post-dates that of rutile, these ages are considered to indicate titanite growth under medium- to high-grade conditions, possibly in association with the event that formed the coexisting low-U zircons. The rutile fraction, with a younger  $^{206}\text{Pb}/^{238}\text{U}$  age of 372 Ma, is considered to represent a cooling age below the closure temperature.

In the eclogite facies paragneiss (Fig. 4b), the two titanite fractions analysed yield data points with poor precision owing to the high initial common Pb content (5–7 ppm) probably related to the abundant tiny opaque inclusions (see above). However, the two fractions overlap one another and yield  $^{206}\text{Pb}/^{238}\text{U}$  ages of 402 and 404 Ma, consistent with the  $^{207}\text{Pb}/^{235}\text{U}$  age of a coexisting monazite single grain, and suggest that this age represents the time of simultaneous titanite and monazite growth in this gneiss. This is supported by petrographic evidence indicating that titanite growth was coeval with the development of the Early Variscan foliation.

### Geological significance of U–Pb ages

In this section we will discuss the main implications of the U–Pb data for the geological evolution of the HP HT units within the Allochthonous Complexes of NW Iberia. The discussion will be aimed at providing hypotheses, ideas and some conclusions regarding the main objectives we set out to accomplish with this geochronological work.

In our view, the main outcome of this research is that the new data clearly reveal that the HP HT units in the NW Iberian Massif record a polyorogenic evolution with (at least) two metamorphic episodes in the Early Ordovician and the Early Devonian, respectively, separated by a ca. 100-million-year period of which there remains a very poor (or non-existent) U–Pb isotopic record. This first order conclusion contrasts with previous research that favoured the existence of only one metamorphic episode (either Devonian or Ordovician).

#### The Early Ordovician event

The Early Ordovician event is recorded by concordant monazite and zircon ages in metasediments. Zircons

with inherited Precambrian components also yield discordias with Early Ordovician lower intercepts. According to the monazite U–Pb data reported herein (Table 1, Figs. 4, 5, 6, 7, 8 and 9), this event had its acme between 485 and 495 Ma. However, the event might have started at ca. 500 Ma ( $^{207}\text{Pb}/^{206}\text{Pb}$  age of a slightly discordant multigrain fraction in sample 11). This age span is analytically indistinguishable from that obtained by Abati et al. (1999) by U–Pb dating of monazite in intermediate-pressure granulites from the overlying uppermost units of the Ordenes Complex (ca. 485–498 Ma).

The zircon ages in the metasediments (samples GCH-99-1 and -17) are younger than the monazite ages and, as claimed above, they represent an event of zircon growth at ca. 470–480 Ma. Although the data do not allow us to place finer constraints on the duration of this event it can be said with confidence that it post-dates the acme of monazite growth by ca. 5 to 10 million years. Some authors (e.g. Mezger and Krogstad 1997, and references therein) question the validity of lower intercept ages if they are younger than those of monazite, and suggest that they should be taken as minimum age constraints. However, in the present case, the finding of a sub-concordant fraction with a maximum age of  $481 \pm 3$  Ma in sample GCH-99-1 supports our view that zircon growth locally post-dates the growth of monazite.

A later growth of zircon than of monazite implies that these minerals image different sections of the P–T trajectory of the rocks. Zircon growth in high-grade metamorphic rocks may not necessarily date the peak P–T conditions as often assumed, but rather a subsequent stage along the decompression path of the P–T trajectory (cf. Wendt et al. 1993; Roberts and Finger 1997) in which zircon growth is related to the presence of a melt phase in the rock. In the present study, both paragneiss samples show evidence of melting and in both all the Zr would have been tied up in detrital zircons, thus making it difficult for new zircon to form in a subsolidus environment. Thus, we propose that monazite ages date the peak conditions (or are closer to them) at ca. 485–495 Ma whereas zircon growth occurred during a stage of decompression accompanied by melt formation.

The crystallisation age of  $486 \pm 4$  Ma of the leucosome within the retrogressed mafic granulite is further evidence in favour of fast decompression following peak granulite-facies conditions. In addition, this datum strongly supports that the HP granulite to eclogite-facies metamorphism recorded by the HP HT units is Early Ordovician in age. The crystallisation age of the leucosome is identical to that yielded by a Sm–Nd (whole rock garnet clinopyroxene) isochron in a clinopyroxenite from the Bragança complex, which provided an age of  $485 \pm 17$  Ma (Santos 1998), and suggests contemporaneity of crustal and mantle melting (or rather the crust lithospheric mantle ensemble) after peak granulite eclogite-facies metamorphism.

A relevant question that arises from the above discussion is whether granulite to eclogite-facies conditions

could have been sustained for a period of ca. 100 million years into the Devonian. This seems unlikely as the preservation of high-pressure relics implies rapid exhumation/uplift after attainment of peak conditions (e.g. Platt 1993).

The above arguments also reopen the question of whether or not all the Early Ordovician ages obtained by SHRIMP in allegedly magmatic domains of zircons (see introductory sections above) from mafic granulites and eclogites represent actual magmatic crystallisation ages or whether they represent ages of metamorphic growth. In fact, some of the U Pb dates claimed to be magmatic protolith ages in mafic granulites and eclogites are younger than monazite ages in the HP HT metasediments.

Finally, we must comment on the possible geodynamic scenario in which these events occurred. Recently, Abati et al. (1999) and Abati (2000) have proposed that the upper units of the AC were formed at a convergent plate boundary, possibly a volcanic arc setting. They base the hypothesis on the general character of the magmatic and metamorphic evolution and the metamorphic gradients that display many common features with modern arcs. They propose a scenario in which the emplacement of ca. 500-Ma-old gabbros and granitoids at shallow crustal levels is followed shortly by their burial and regional metamorphism from granulite-facies conditions in the IP units and granulite to eclogite facies conditions in the HP HT units. According to the data presented herein, these units might have undergone rapid exhumation after burial. The palaeogeography of this alleged arc in the context of the Laurentia Gondwana interactions during the Early Palaeozoic has been discussed by, for example, Martínez Catalán et al. (1999) and Abati et al. (1999). The present study does not (and did not aim to) furnish new data in this regard, but it does strengthen the hypothesis that the tectono-thermal evolution of the upper units of the AC in NW Iberia is compatible with an (Early Palaeozoic) island arc scenario in which magmatism, burial metamorphism with high T gradients and fast exhumation are common features (e.g. Hiroi et al. 1998).

### The Early Devonian event

A ca. 100-Ma-younger Early Devonian event is recorded by monazite, titanite and rutile concordant ages in metasediments of the HP HT units. However, the imprint of this second event is not observable in all samples and it appears in different ways in the samples where it is registered by the U Pb isotopic system. Direct evidence for this event is found in samples GCH-99-1, -9, and -13, and it is interpreted to be present in sample 7 (see discussion in previous section). The analytical data presented in this work suggest that this event reached its acme in an age span of some 5 million years between 385 and 390 Ma, but it might have started at ca. 400–405 Ma, in agreement with data obtained in other units of the

Allochthonous Complexes (Santos Zalduegui et al. 1996). These ages are also in agreement with SHRIMP data on U-rich, CL-structureless rims of zircons from metasediments of these units (Ordóñez Casado 1998). The age interval revealed by the present U Pb work also matches a number of ages obtained on zircons (IDTIMS and SHRIMP) monazites and titanites (IDTIMS) from a variety of rocks from the upper units of the AC representing both mantle and crustal melts (Peucat et al. 1990; Schäfer et al. 1993; Santos Zalduegui et al. 1996; Ordóñez Casado 1998). In addition, this age interval is coeval with the age of retrograde amphibolite facies metamorphism proposed for the HP HT units on the basis of  $^{40}\text{Ar}$ – $^{39}\text{Ar}$  dating of fabrics (Dalhneier and Gil Ibarguchi 1990; Peucat et al. 1990; Dallmeyer et al. 1991; Dallmeyer et al. 1997). Dallmeyer et al. (1997) obtained a plateau hornblende  $^{40}\text{Ar}$ – $^{39}\text{Ar}$  age of 425 Ma in a retrograded mafic granulite from the Ordenes Complex. They considered the significance of this datum to be uncertain given that, at that point, the HP HT metamorphism was being interpreted as Early Devonian in age. This datum is now more easily interpretable within the framework of an Early Ordovician age of the HP HT metamorphism as it can then be interpreted to represent a cooling age from peak or post-peak granulite conditions.

Another relevant aspect of this work is that it shows that the Early Devonian effects are recorded in different ways in different units, being more intense in those rocks located in areas of more intense Variscan tectono-thermal reworking. This is particularly evident in samples 7 and 13 (Figs. 5 and 8), both located within Variscan shear zones. In this respect, it is important to note that monazites in sample GCH-99-13 yield an average age of 386 Ma (Fig. 8). The sample is located immediately below the Corredoiras Detachment (Díaz García et al. 1999a), previously dated at 375 Ma ( $^{40}\text{Ar}/^{39}\text{Ar}$  on hornblende concentrates; Dallmeyer et al. 1997). This episode was apparently not recorded by the U Pb system in areas situated outside zones of intense Variscan tectonic activity. This is also consistent with the data provided by Abati et al. (1999) in the structurally overlying intermediate-pressure units, where U Pb dating of monazite from metasediments did not reveal the presence of the Early Devonian component.

These aspects are of importance when attempts are made at constraining the nature and conditions of the Early Devonian metamorphic event. As we have stated, some authors claim that this episode was the HP HT granulite to eclogite single metamorphic event related to a single subduction event in Early Devonian times. In previous sections we have defended the hypothesis that the HP HT event is Early Ordovician and was possibly generated in an arc environment in a peri-Gondwanan ocean reahn. If so, what is the nature and setting of the 385–395 Ma event? From data obtained in this work, we know that this event produced growth of new monazite and growth of titanite in the metasediments and in the leucosome. However, this does not give an indication of

T because both minerals can grow in relatively low T environments in the presence of a fluid phase. On the other hand, we know from independent criteria that this event (at least locally) was high-grade enough to melt mantle and crustal rocks involved in the Variscan Collision (Santos Zalduegui et al. 1996). Also, we argue that the evidence for this event, at variance with the Early Ordovician event, is localised in zones of Variscan tectonic reworking. The ages presented in this work are in agreement with the model proposed by Martínez Catalán et al. (1997, 1999) according to which the HP HT units were variously deformed during their emplacement onto the structurally underlying ophiolitic units in the early stages of the Variscan Laurentia Gondwana collision (ca. 390–380 Ma). In this scenario, growth of titanite and monazite might have been enhanced in highly strained rocks within shear zones by the action of fluid circulation. Similar cases of growth or resetting of U-bearing minerals in fluid-rich high-strain environment are reported in many areas (e.g. Tucker et al. 1987; Gromet 1991; Ketchum et al. 1998). This would also be consistent with the formation of CL structureless rim domains in some zircons that yield SHRIMP U–Pb ages at ca. 380–390 Ma (Schäfer et al. 1993; Ordóñez Casado 1998). We suggest, therefore, that the Early Devonian event was not a HP event in the upper units of the Allochthonous Complexes, but was generated in a general context of crustal deformation in the overriding terrane during the early stages of Variscan collision that involved underthrusting of the outer edge of Gondwana and HP metamorphism in the basal units broadly coeval with the Early Devonian event, here studied in the upper units.

A few words must also be said regarding the apparent ca. 100-million-year gap separating the two metamorphic events. Although some ages intermediate between 480–490 and 380–390 were obtained in single monazite grains and zircon multigrain fractions, we believe that they most likely represent either mixing of Ordovician and Devonian components or differential lead-loss and there is no solid geochronological evidence arising from our data to suggest that they might represent an actual geologic event or events. Neither have other isotopic systems (Sm–Nd, Ar–Ar or Rb–Sr) provided solid evidence in favour of the existence of high-grade events in that time gap.

## Conclusions

The HP HT units were possibly generated at a convergent plate boundary in a yet unconstrained realm of the Rheic Ocean domain where arc-type magmatism, sedimentation and ‘quick burial’ high-pressure metamorphism followed by fast exhumation took place in a time span that, with available data, can be constrained between ca. 500 and 470 Ma. The ensemble thus generated was subsequently involved in the Variscan (Laurentia–Gondwana) collision. The 380–390-Ma event was possibly related to the emplacement of the upper units onto

the ophiolites, which, at that time, were being underthrust and stacked during the closure of the intervening ocean (Martínez Catalán et al. 1997, 1999).

The above data and discussion, although mainly of regional significance, also bear some relevance to the always delicate and exacting task of dating tectonothermal events in polyorogenic terranes. In this regard, our work contributes to strengthen the idea that such studies should not rely on one single mineral, and that the ideal case is one in which information can be obtained from minerals with different isotopic response to the P–T evolution of the rock. Moreover, one should be aware that a sufficient number of samples must be studied in order not to get a biased or dangerously incomplete image of the events. In other words, in terranes with complex tectonometamorphic histories one must make sure that the rocks studied are actually representative of the geological events one is trying to study through a geochronological approach.

**Acknowledgements** This research was funded by PB97-0234-C02 project to José Ramón Martínez Catalán and Ricardo Arenas, and PB98 1545 project to Alberto Marcos. J.F.S. wishes to acknowledge a Contrato de Reincorporación para Doctores y Tecnólogos granted by the Spanish Ministry of Education. Gunborg Bye-Fjeld is kindly acknowledged for her assistance in the mineral separation laboratory. Mark Schmitz and an anonymous referee are thanked for constructive and insightful reviews.

## References

- Abati J (2000) Petrología metamórfica y geocronología de la unidad culminante del complejo de Ordenes en la región de Carballo (Galicia, NW del Macizo Ibérico). PhD Thesis, Universidad Complutense, Madrid
- Abati J, Dunning GR, Arenas R, Díaz García F, González Cuadra P, Martínez Catalán JR (1999) Early Ordovician orogenic event in Galicia (NW Spain): evidence from U–Pb ages in the uppermost unit of the Ordenes Complex. *Earth Planet Sci Lett* 165:213–228
- Arenas R, Martínez Catalán JR (1993) High-pressure and high-temperature metabasites from the Sobrado antiform (northwest of the Iberian Massif, Spain). *Terra Abstr* 4: 5–2
- Arenas R, Rubio Pascual FJ, Díaz García F, Martínez Catalán JR (1995) High-pressure micro-inclusions and development of an inverted metamorphic gradient in the Santiago Schists (Ordenes Complex, NW Iberian Massif, Spain): evidence of subduction and syn-collisional decompression. *J Metamorph Geol* 13:141–164
- Arenas R, Abati J, Martínez Catalán JR, Díaz García F, Rubio Pascual FJ (1997) P–T evolution of eclogites from the Agualada unit (Ordenes Complex, NW Iberian Massif, Spain): implications for crustal subduction. *Lithos* 40:221–242
- Arenas R, Martínez Catalán JR (2000) Prograde development of corona textures in metagabbros of the Sobrado Window (Ordenes Complex, NW Iberian Massif). In: Variscan Appalachian dynamics: the building of the Upper Paleozoic basement. *Basement tectonics*, vol 15, program and abstracts. A Coruña, Spain, pp 42–45
- Corfu F, Stott GM (1986) U–Pb ages for late magmatism and regional deformation in the Shebandowan belt, Superior Province, Canada. *Can J Earth Sci* 23:1075–1082
- Crowley JL, Ghent ED (1999) An electron microprobe study of the U–Th–Pb systematics of metamorphosed monazite: the role of Pb diffusion versus overgrowth and recrystallisation. *Chem Geol* 157:285–302



- Dallmeyer RD, Gil Ibarra JI (1990) Age of amphibolitic metamorphism in the ophiolitic unit of the Morais allochthon (Portugal): implications for early Hercynian orogenesis in the Iberian Massif. *J Geol Soc Lond* 147:873-878
- Dalhneier RD, Tucker RD (1993) U-Pb zircon age for the Lagoa augen gneiss, Morais complex, Portugal: tectonic implications. *J Geol Soc* 150:405-410
- Dalhneier RD, Ribeiro A, Marques F (1991) Polyphase Variscan emplacement of exotic terranes (Morais and Bragança Massifs) onto Iberian successions: evidence from  $^{40}\text{Ar}/^{39}\text{Ar}$  mineral ages. *Lithos* 27:133-144
- Dalhneier RD, Martínez Catalán JR, Arenas R, Gil Ibarra JI, Gutiérrez Alonso G, Fariás P, Basáñez F, Aller J (1997) Diachronous Variscan tectonothermal activity in the NW Iberian Massif: evidence from  $^{40}\text{Ar}/^{39}\text{Ar}$  dating of regional fabrics. *Tectonophysics* 277:307-337
- Díaz García F, Martínez Catalán JR, Arenas R, González Cuadra P (1999a) Structural and kinematic analysis of the Corredoiras detachment: evidence for Early Variscan synconvergent extension in the Ordenes Complex, NW Spain. *Int J Earth Sci* 88:337-351
- Díaz García F, Arenas R, Martínez Catalán JR, González del Tánago J, Dunning GR (1999b) Tectonic evolution of the Careón ophiolite (northwest Spain): a remnant of oceanic lithosphere in the Variscan belt. *J Geol* 107:587-605
- Galán G, Marcos A (1997) Geochemical evolution of high-pressure mafic granulites from the Barcariza formation (Cabo Ortegal complex, NW Spain): an example of a heterogeneous lower crust. *Geol Rundsch* 86:539-555
- Galán G, Marcos A (2000) The metamorphic evolution of the high-pressure mafic granulites of the Barcariza Formation (Cabo Ortegal Complex, Hercynian belt, NW Spain). *Lithos* 54:139-171
- Gil Ibarra JI, Mendia M, Girardeau J, Peucat JJ (1990) Petrology of the eclogites and the clinopyroxene garnet metabasites from the Cabo Ortegal complex (northwest Spain). *Lithos* 25:133-162
- Girardeau J, Gil Ibarra JI (1991) Pyroxene-rich peridotites of the Cabo Ortegal Complex (northwest Spain): evidence for a large-scale upper-mantle heterogeneity. *J Petrol* 32:135-154
- Gromet LP (1991) Direct dating of deformational fabrics. In: Heaman L, Ludden J (eds) Applications of radiogenic isotope systems to problems in geology. Short course handbook 19. Mineralogy Association of Canada, Ottawa, pp 167-189
- Hawkins DP, Bowring SA (1997) U-Pb systematics of monazite and xenotime: case studies from the Paleoproterozoic of the Grand Canyon, Arizona. *Contrib Mineral Petrol* 127:87-103
- Hiroi Y, Kishi S, Nohara T, Sato K, Goto J (1998) Cretaceous high-temperature rapid loading and unloading in the Abukuma metamorphic terrane, Japan. *J Metamorph Geol* 16:67-81
- Ketchum JWF, Heaman LM, Krogh TE, Culshaw NG, Jamieson RA (1998) Timing and thermal influence of late orogenic extension in the lower crust: a U-Pb geochronological study from the southwest Grenville orogen, Canada. *Precambrian Res* 89:25-45
- Krogh TE (1982) Improved accuracy of U-Pb ages by the creation of more concordant systems using an air abrasion technique. *Geochim Cosmochim Acta* 46:637-649
- Kuijper RP (1979) U-Pb systematics and the petrogenetic evolution of infracrustal rocks in the Paleozoic basement of western Galicia (NW Spain). PhD Thesis, ZWOL Laboratory of Isotope Geology, Amsterdam
- Jaffey AH, Flynn KF, Glendenin LE, Bentley WC, Essling AM (1971) Precision measurements of half-lives and specific activities of  $^{235}\text{U}$  and  $^{238}\text{U}$ . *Phys Rev C, Nucl Phys* 4:1889-1906
- Ludwig KR (1989) Pb.dat: a computer program for processing raw Pb-U-Th isotope data. *US Geol Surv Open-File Rep* 88-557
- Ludwig KR (1998) On the treatment of concordant uranium-lead ages. *Geochim Cosmochim Acta* 62:665-676
- Martínez Catalán JR, Arenas R (1992) Deformación extensional de las unidades alóctonas superiores de la parte oriental del complejo de Ordenes (Galicia). *Geogaceta* 11:108-111
- Martínez Catalán JR, Arenas R, Díaz García F, Rubio Pascual FJ, Abati J, Marquínez J (1996) Variscan exhumation of a subducted Paleozoic continental margin: the basal units of the Ordenes Complex, Galicia, Spain. *Tectonics* 15:106-121
- Martínez Catalán JR, Arenas R, Díaz García F, Abati J (1997) The Variscan accretionary complex of NW Iberia: involved terranes and succession of tectonothermal events. *Geology* 25:1103-1106
- Martínez Catalán JR, Arenas R, Díaz García F, Abati J (1999) Allochthonous units in the Variscan belt of NW Iberia. In: Sinha AK (ed) Basement Tectonics 13:65-84
- Mendia M (1996) Petrología de la unidad eclogítica del complejo de Cabo Ortegal (NW de España). PhD Thesis, Universidad del País Vasco
- Mezger K, Krogstad EJ (1997) Interpretation of discordant U-Pb zircon ages: an evaluation. *J Metamorph Geol* 15:127-140
- Ordóñez Casado B (1998) Geochronological studies of the pre-Mesozoic basement of the Iberian Massif: the Ossa Morena zone and the Allochthonous Complexes within the Central Iberian Zone. PhD Thesis, ETH, Zurich
- Parrish RR (1990) U-Pb dating of monazite and its application to geological problems. *Can J Earth Sci* 27:1431-1450
- Peucat JJ, Bernard-Griffiths J, Gil Ibarra JI, Dallmeyer RD, Menot RP, Cornichet J, Iglesias Ponce de León M (1990) Geochemical and geochronological cross-section of the deep Variscan crust: the Cabo Ortegal high-pressure nappe (northwestern Spain). *Tectonophysics* 177:263-292
- Platt J (1993) Exhumation of high-pressure rocks: a review of concepts and processes. *Terra Nova* 5:2:119-133
- Roberts MP, Finger F (1997) Do U-Pb zircon ages from granulites reflect peak metamorphic conditions? *Geology* 25:319-322
- Santos JF (1998) Geoquímica de litologías básicas e ultrabásicas da unidade alóctone superior do Maciço de Bragança. PhD Thesis, Universidade de Aveiro, Portugal
- Santos Zalduegui JF, Schärer U, Gil Ibarra JI, Girardeau J (1996) Origin and evolution of the Paleozoic Cabo Ortegal ultramafic-mafic complex (NW Spain): U-Pb, Rb-Sr and Pb-Pb isotope data. *Chem Geol* 129:281-304
- Schärer HJ, Gebauer D, Gil Ibarra JI, Peucat JJ (1993) Ion-microprobe U-Pb zircon dating on the HP/HT Cabo Ortegal complex (Galicia, NW Spain): preliminary results. *Terra Abstr* 5:4:22
- Schärer U (1984) The effect of initial  $^{230}\text{Th}$  disequilibrium on young U-Pb ages: the Makalu case, Himalaya. *Earth Planet Sci Lett* 67:191-204
- Simpson RL, Parrish RR, Searle MP, Waters DJ (2000) Two episodes of monazite crystallisation during metamorphism and crustal melting in the Everest region of the Nepalese Himalaya. *Geology* 28:403-406
- Stacey JS, Kramers JD (1975) Approximation of terrestrial lead isotope evolution by a two stage model. *Earth Planet Sci Lett* 26:207-221
- Tucker RD, Raheim A, Krogh TE, Corfu F (1987) Uranium-lead zircon and titanite ages from the northern portion of the Western Gneiss Region, south-central Norway. *Earth Planet Sci Lett* 81:203-211
- Vavra G, Schaltegger U (1999) Post-granulite facies monazite growth and rejuvenation during Permian to Lower Jurassic thermal and fluid events in the Ivrea Zone (Southern Alps). *Contrib Mineral Petrol* 134:405-414
- Vogel DE (1967) Petrology of an eclogite- and pyroxenite-bearing polymetamorphic rock complex at Cabo Ortegal, NW Spain. *Leids Geol Mededelingen* 40:121-213
- Wendt JI, Kröner A, Fiala J, Todt W (1993) Evidence from zircon dating for existence of approximately 2.1 Ga old crystalline basement in southern Bohemia, Czech Republic. *Geol Rundsch* 82:42-50
- Zhu XK, O'Nions RK (1999) Zonation of monazite in metamorphic rocks and its implications for high temperature thermochronology: a case study from the Lewisian terrain. *Earth Planet Sci Lett* 171:209-220